Title
Effect of Polymer Hydration State on In-Gel Immunoassays

Journal
Analytical Chemistry, 87(21)

ISSN
0003-2700

Authors
Vlassakis, Julea
Herr, Amy E

Publication Date
2015-11-03

DOI
10.1021/acs.analchem.5b03032

Peer reviewed

analytical chemistry

Article

pubs.acs.org/ac

Effect of Polymer Hydration State on In-Gel Immunoassays

Julea Vlassakis and Amy E. Herr*

Department of Bioengineering and The UC Berkeley/UCSF Graduate Program in Bioengineering, University of California Berkeley, Berkeley, California 94720, United States

Supporting Information

ABSTRACT: Applications as diverse as drug delivery and immunoassays require hydrogels to house high concentration macromolecular solutions. Yet, thermodynamic partitioning acts to lower the equilibrium concentration of macromolecules in the hydrogel, as compared to the surrounding liquid phase. For immunoassays that utilize a target antigen immobilized in the hydrogel, partitioning hinders introduction of detection antibody into the gel and, consequently, reduces the in-gel concentration of detection antibody, adversely impacting assay sensitivity. Recently, we developed a single-cell targeted proteomic assay with polyacrylamide gel electrophoresis of single cell lysates followed by an in-gel immunoassay. In the present work, we overcome partitioning that both limits analytical sensitivity and increases consumption of costly detection antibody by performing the immunoassay step after dehydrating the antigen-containing polyacrylamide gel. Gels are rehydrated with a solution of detection antibody. We hypothesized that matching the volume of detection antibody solution with the hydrogel water volume fraction would ensure that, at equilibrium, the detection antibody mass resides in the gel and not in the liquid surrounding the gel. Using this approach, we observe (compared with antibody incubation of hydrated gels): (i) 4−11 fold higher concentration of antibody in the dehydrated gels and in the single-cell assay (ii) higher fluorescence immunoassay signal, with up to 5-fold increases in signal-to-noise-ratio and (iii) reduced detection antibody consumption. We also find that detection antibody signal may be less well-correlated with target protein levels (GFP) using this method, suggesting a trade-off between analytical sensitivity and variation in immunoprobe signal. Our volume-matching approach for introducing macromolecular solutions to hydrogels increases the local in-gel concentration of detection antibody without requiring modification of the hydrogel structure, and thus we anticipate broad applicability to hydrogel-based assays, diagnostics, and drug delivery.

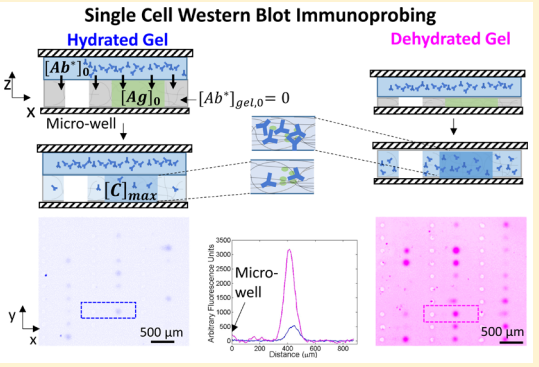

For applications spanning from macromolecule release (e.g., drug delivery[1−4]) to detection (e.g., immunoassays[5−7]), thermodynamic partitioning hinders diffusive entry of macromolecules into a wetted hydrogel. For "in-gel" immunoassays where target is immobilized in a hydrogel, detection antibodies applied to the gel partition between the gel and free-solution phase. We can describe the partitioning of detection antibodies (Ab*, where the asterisk (*) indicates detection probe is labeled with a fluorophore) with an in-gel Ab* concentration $[Ab^*]_{gel}$ given by

$$[Ab^*]_{gel} = K_{partition} \times [Ab^*]_0 \quad (1)$$

where $K_{partition}$ is the equilibrium partition coefficient and $[Ab^*]_0$ is the solution concentration of antibody. A $K_{partition} < 1.0$ indicates an in-gel macromolecule concentration lower than the solution phase concentration. Partitioning arises from both size-exclusion and macromolecule interactions with the hydrogel and solvent, including hydrophobic−hydrophobic and electrostatic interactions.[8,9] The equilibrium in-gel concentration of macromolecule may be lowered by up to 1000-fold from the starting solution concentration.[8,9] As a result, numerous approaches aim to alter the partition coefficient with addition of salts or molecules such as PEG[10−12] to the solution or hydrogel. Another class of approaches actively loads the hydrogel with macromolecule using mechanical or electrical forces.[13,14] Such methods increase in-gel macromolecule concentrations by over 10-fold, with utility dependent on scalability and compatibility with the specific drug delivery or immunoassay system. As a result, more generalizable approaches to overcome partitioning for hydrogel loading would prove useful.

Low in-gel concentrations of detection antibody can reduce the analytical sensitivity of an immunoassay even with a high density of immobilized target (e.g., in a 3D hydrogel matrix).[15−17] On the basis of bimolecular binding kinetics, the maximum immunocomplex formed by the reaction of detection antibody with target antigen (Ag) is given by

Received: August 7, 2015
Accepted: October 12, 2015
Published: October 12, 2015

DOI: 10.1021/acs.analchem.5b03032
Anal. Chem. 2015, 87, 11030−11038

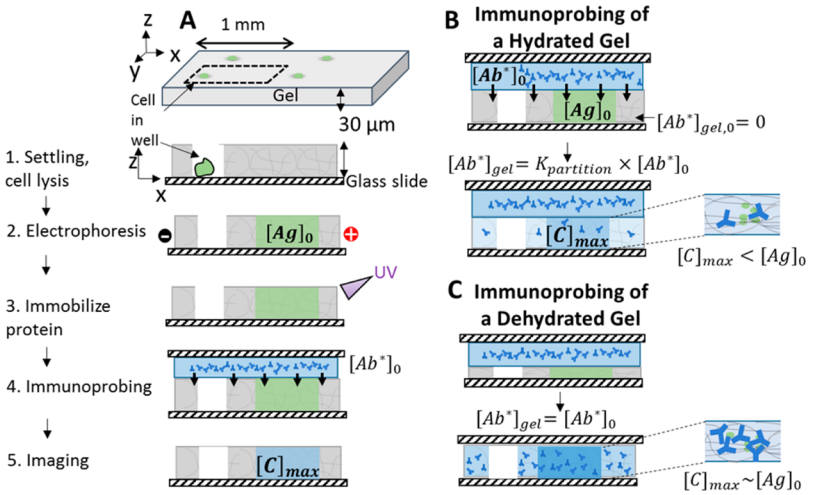

Figure 1. In-gel immunoassays are affected by preferential partitioning of detection antibody out of the hydrogel and into a solution phase as is relevant to the immunoprobing step in single-cell Western blotting. (A) The scWB utilizes a thin layer of micropatterned PA gel attached to a microscope slide with an assay workflow that consists of (1) settling and lysis of single cells in microwells cast into the PA gel layer, (2) PA gel electrophoresis (PAGE) of each single-cell lysate in the supporting PA gel layer, (3) UV immobilization of protein in the gel, (4) in-gel immunoprobing using fluorescently labeled detection antibodies ($[Ab^*]_{gel}$), and (5) fluorescence imaging. (B) Schematic of immunoprobing in a hydrated gel, including diffusion and partitioning of detection antibody and immobilized protein target, $[Ag]_0$. Partitioning lowers the in-gel concentration of detection antibody, $[Ab^*]_{gel}$, at equilibrium thus yielding $[C]_{max} < [Ag]_0$. (C) Schematic of immunoprobing by rehydrating a dehydrated gel with a matched volume of detection antibody solution. A dried gel is rehydrated with a volume of detection antibody on the order of the hydrogel water volume fraction, such that at equilibrium, the majority of the detection antibody is located in the gel, which drives immunocomplexation to saturation thus yielding $[C]_{max} \approx [Ag]_0$.

$$[C]_{max} = \frac{k_{on}[Ab^*]_{gel}[Ag]_0}{k_{on}[Ab^*]_{gel} + k_{off}} \quad (2)$$

where $[Ag]_0$ is the target protein concentration, k_{on} (M^{-1} s^{-1}) is the association rate constant, and k_{off} (s^{-1}) is the dissociation rate constant. Thus, for in-gel immunoassays, the maximum immunocomplex formation and analytical sensitivity depends on the local concentration of detection antibody in the gel.

Enhancing the analytical sensitivity of an in-gel immunoassay is an outstanding analytical challenge in the single-cell Western blot (scWB) format we recently introduced.[18] Existing single cell proteomic measurements such as immunocytochemistry, flow cytometry and other immunoassay based methods[19−26] have provided fundamental insight into the heterogeneity of protein expression driving cancer[25] and stem cell differentiation.[27] However, nonspecific antibody binding has been implicated in false signal and incorrect localization, necessitating the development of the scWB.[28,29] The scWB utilizes a microfabricated polyacrylamide (PA) hydrogel for single-cell protein electrophoresis, covalent photoimmobilization of protein bands to the gel, and subsequent immunoprobing (Figure 1A).[18,30] Single-cell electrophoresis identifies off-target antibody binding and protein isoforms.[18] We perform immunoprobing in the separation gel by diffusively introducing primary and then fluorescently labeled secondary antibodies (Figure 1B). During immunoprobing in the PA gel thermodynamic partitioning lowers $[Ab^*]_{gel}$ and, thus, the analytical sensitivity of the assay.[18,30] In the scWB, we observed $K_{partition} \approx 0.17$ (8%T gel) meaning that just ∼17% of the applied concentration of detection antibody will be in-gel at equilibrium.[18] Antibody size-exclusion from the dense molecular sieving gel occurs even though the hydrodynamic radius of an IgG antibody is ∼5 nm[31] and estimates of average PA gel pore size are ∼50−90 nm for a 7−8% T (total monomer concentration) gel (with 3−4% C, percent bis-acrylamide cross-linker).[32] While reducing the gel density (and increasing the gel pore-size) would increase the partition coefficient, the resolving performance of protein electrophoresis would be reduced. Low in-gel concentrations of detection antibody reduce the immunocomplex formed at equilibrium, thus impacting analytical sensitivity for certain targets. Consequently, immunoprobing of the scWB requires higher antibody consumption than competing single-cell technologies including flow cytometry.[33]

To overcome partitioning limitations for in-gel immunoassays, we introduce a detection antibody loading method based on rehydration of hydrogels (in which protein is immobilized) with a volume of detection antibody solution closely matched to the water volume fraction of the hydrogel. This yields near-bulk concentrations of antibody in the gel. To our knowledge, this is the first report of matched volume gel rehydration as a mechanism to reduce the solution phase volume and macromolecular partitioning into the solution phase and to enhance the in-gel concentration of detection antibody. Here for the scWB, we demonstrate reduced detection antibody consumption and increased detection signal from in-gel immunoassays for protein targets with a trade-off in spatial signal variation.

EXPERIMENTAL SECTION

Chemicals/Reagents. Acetic acid (A6283), 3-(trimethoxysilyl)propyl methacrylate (662275), 30% T, 3.4% C acrylamide/bis-acrylamide (29:1) (A3574), *N,N,N′,N′*-tetramethylethylenediamine (TEMED, T9281), bovine serum albumin (BSA, A7030), ammonium persulfate (APS, A3678), sodium deoxycholate (D6750), and sodium dodecyl sulfate (SDS, L4509) were purchased from Sigma-Aldrich. Triton X-100 (BP-151) was attained from ThermoFisher Scientific. Tris-buffered saline with tween (20× TBST, 281695) was acquired from Santa Cruz Biotechnology. Premixed 10× Tris/glycine

DOI: 10.1021/acs.analchem.5b03032
Anal. Chem. 2015, 87, 11030−11038

electrophoresis buffer (25 mM Tris, pH 8.3; 192 mM glycine) was procured from BioRad. Phosphate buffered saline (10X PBS, 45001−130) was purchased from VWR International. Deionized water (18.2 MΩ) was obtained using an Ultrapure water system from Millipore. *N*-[3-[(3-Benzoylphenyl)-formamido]propyl] methacrylamide (BPMAC) was custom synthesized by PharmAgra Laboratories. Lentiviral infection (multiplicity of 10) was performed to produce U373 MG cells expressing Turbo GFP, which were generously provided by Dr. Ching-Wei Chang in Prof. S. Kumar's Laboratory. Rabbit anti-Turbo GFP antibodies (PA5-22688) were acquired from Pierce Antibody Products. Donkey antirabbit Alexa-Fluor 647-labeled secondary antibodies (A31573) were procured from Invitrogen. Recombinant Turbo GFP (FP552) was obtained from Evrogen.

Cell Culture. The U373-GFP cells were cultured in a humidified 37 °C incubator kept at 5% CO_2 with high glucose DMEM media (11965, Life Technologies) containing high glucose DMEM (11965, Life Technologies) supplemented with 1× MEM nonessential amino acids (11140050, Life Technologies), 1% penicillin/streptomycin (15140122, Invitrogen), 1 mM sodium pyruvate (11360−070, Life Technologies), and 10% calf serum (JR Scientific) in a humidified 37 °C incubator with 5% CO_2.

Hydration Kinetics Experiments. PA gels were dried in a nitrogen stream for ∼1 min. Dry gel mass was measured on an analytical balance (Ohaus, DV215CD), and gels were rehydrated in 1X TBST buffer. Upon removal of the gel from the TBST, gels were blotted dry using Kimwipes and weighed.

In-Gel Antibody Concentration Quantitation Experiments. PA gels with benzophenone methacrylamide incorporated (7%T, 3 mM BPMAC) without microwells or protein immobilized were fabricated as described elsewhere[18] for the in-gel antibody concentration quantitation experiments. The experiments were performed with antibody solution in excess volume (15 mL of 0.02 mg/mL fluorescent secondary Ab) or approximately the gel hydration volume (50 μL for dehydrated gels, 25 μL for hydrated gels; 0.02 mg/mL concentration, 0.5 μg of antibody per half slide). Following 1 h antibody incubation, antibody was immobilized in the gel using the benzophenone capture reaction upon UV exposure (OAI Model 30 Collimated UV Light Source, 25.5 mW/cm^2 for 2 min), and gels were washed in 1× TBST and imaged.

Single Cell Western blots. The scWBs were performed as previously described[18] up until the immunoprobing stage. To study the impact of gel hydration state on in-gel detection antibody concentration, we (i) used diffusive probing of a hydrated gel or (ii) introduced detection antibody solution to a PA gel previously dried with a nitrogen stream (probing of a dehydrated gel), as indicated in the discussion of results. Briefly, the scWB was performed utilizing a PA gel that was grafted to a methacrylate treated glass microscope slide. The microwell array was created by chemically polymerizing a 7%T PA gel precursor solution on an SU-8 mold sandwiched to the glass microscope slide. A cell suspension (∼10^6 cells/mL in 1× PBS) was introduced to the PA gel surface, cells were settled by gravity into the microwells, and excess cells were washed off the gel. Cells were lysed (∼12 s) within the wells in a 1× modified RIPA buffer,[18] and the proteins were electrophoresed into the gel at ∼40 V/cm (∼25s) in a custom electrophoresis chamber. The proteins were immediately photoimmobilized in the gel by a UV-mediated covalent reaction between abstractable hydrogens[34] on the proteins and the BPMAC groups incorporated in the gel matrix (Lightningcure LC5, Hamamatsu, 100% power 45 s exposure). At the immunoassay step, antibody in 1× TBST with 5% BSA (25 μL per half slide for immunoprobing of hydrated gels, 50 μL per half slide for immunoprobing of dehydrated gels was loaded at the edge of the gel and sandwiched between the gel and another glass slide. Immunoprobing of hydrated and dehydrated gels proceeded for 2 h (primary antibody), and for 1 h with secondary antibody. Gels were washed two times in 1× TBST for 30 min each on an orbital shaker between probing steps. Imaging was performed on a fluorescence microarray scanner (Genepix 4300A, Molecular Devices) with filter sets for the GFP and AlexaFluor 647-labeled antibodies chosen to minimize spectral cross-talk between the fluorescent protein and antibody used to detect the GFP.

Image Analysis and Quantitation. Analysis of scWB images was performed using custom scripts in ImageJ and Matlab. Area under the curve (A.U.C.) fluorescence was calculated by curve-fitting the scWB bands (both the detection antibody and expressed Turbo GFP fluorescence bands) to a Gaussian function, and summing the intensity values between approximately three standard deviations of the peak center. A.U.C. was only reported for scWB bands with a Gaussian fit *R*-squared value >0.7, for accurate selection of peak boundaries. Statistical analysis was carried out with custom and existing Matlab functions.

RESULTS AND DISCUSSION

In-Gel Immunoassays in Dehydrated PA Gels. We sought to satisfy two general in-gel immunoprobing design criteria and one additional specific scWB immunoprobing criterion: (i) transport times for detection antibody into the gel that are comparable to or faster than diffusive transport of detection antibody into the gel, (ii) in-gel concentrations of detection antibody that approximate concentrations in the solution phase (Figure 1C), and (iii) reduced scWB consumption of detection antibody mass, as compared to diffusive antibody introduction in hydrated gels. Immunoprobing in the scWB is an immunoassay in a PA gel; the gel also performs molecular sieving during electrophoretic protein sizing (Figure 1A). A PA gel with 7−10% T can resolve the majority of cytosolic proteins (∼15−90 kDa[35] range). However, attaining baseline separation for ∼21 and ∼65 kDa protein targets requires denser gels.[30] Increasing the volume fraction of the polymer even by a factor of 2 can reduce the partition coefficient by over an order of magnitude.[8] As a result, increasing the density of the gel for improved separation performance would dramatically lower the in-gel concentration of antibody. An analytical model of bimolecular binding kinetics (see Supporting Information) showed only 50% of the total possible immunocomplex will form at equilibrium (with typical antigen concentrations from single cells and a low-to-moderate affinity antibody), thus limiting the analytical sensitivity of the assay (Figure 1B).

To overcome the observed mass transport and thermodynamic limitations, we studied swelling of a dehydrated gel during rehydration as a promising mechanism to drive detection antibody into the dense sieving gel (Figure 1C). Maximizing the local concentration of detection antibody ($[Ab^*]_{gel}$ from eq 2) drives immunocomplex formation to saturation with $[C]_{max} \approx [Ag]_0$. We hypothesized that with antibody solution volume closely matched to the volume required to rehydrate the gel, at equilibrium, all antibody mass would be contained in the gel. We determined a procedure for

DOI: 10.1021/acs.analchem.5b03032
Anal. Chem. 2015, 87, 11030−11038

drying and subsequently rehydrating the gel with antibody solution, and we used the rehydration procedure to increase the local concentration of detection antibody in the dehydrated gel compared with a hydrated gel. Furthermore, we evaluated the impact of increased concentration of detection antibody on the *sc*WB immunoassay theoretically (with a binding kinetics model) and in a proof-of-concept demonstration on single GFP-expressing cells with immunoprobing for detection of GFP in dehydrated gels.

Procedure for Drying and Rehydrating the Gel in Antibody Solution. The goal of increasing the local concentration of detection antibody in the gel required a protocol for (i) drying the hydrogel and (ii) rehydrating the gel in antibody solution. We investigated two main approaches for dehydrating the thin 30 μm PA gels grafted to the glass slide: drying in a nitrogen stream or overnight drying in a desiccator. When drying in the nitrogen stream, we observed the gel undergo a transition from initially clear, to briefly opaque and clear again (where opacity is indicative of light scattering off saturated pores[36]). After drying, to confirm the clear gel was in fact dehydrated, we compared the dry mass of the gel after 1 min in the nitrogen stream to that of a gel dried in the nitrogen stream and stored overnight in a desiccator. We observed no difference in the dry gel mass with overnight drying versus drying in the desiccator, suggesting that 1 min in the nitrogen stream was sufficient to dehydrate the gel.

To meet the design specification of near-bulk antibody concentration in-gel at equilibrium (Figure 1C), we determined the volume required to rehydrate a dehydrated gel. Additionally, determining the time scale of rehydration informs the choice of incubation period during immunoprobing of dehydrated gels. To determine the rehydration volume and time scale, we performed gel swelling kinetics experiments, weighing the gel as a function of rehydration time as performed elsewhere[37] and shown in Figure 2. In the "excess volume" method, the gel was submersed in a TBST buffer bath having a volume ~2 orders of magnitude larger than the anticipated water volume fraction of the hydrated polymer.[38] While in the "matched volume" method, 50 μL of TBST (matched to the order of the water volume fraction of the hydrated polymer) was added to the side of the dried gel and spread across the gel with a glass slide (as used in our scWB protocol). Notably, as demonstrated in Figure 2A, when TBST solution containing antibody was added to the dry gel surface, minimal lateral wicking or spreading of the solution across the gel was observed even up to 45 min after addition of the droplet. Thus, another glass slide was used to spread the drop across the top of the dried gel, so as to overcome interfacial surface tension. In both the "excess volume" and "matched volume" methods, ~34 μL of buffer rehydrated the PA gels, with most rehydration occurring within ~1 s and completing in ~10 s (Figure 2C). Swelling of gels anchored to a glass slide is less than swelling of nonsurface constrained gels.[39] However, the rehydration volume of 34 μL is within 10% of the anticipated rehydration volume for a gel of this geometry and composition (water volume fraction of ~0.96[38]). Similarly, the rehydration time scale corroborates studies of surface-constrained *N*-isopropylacrylamide gels (height, $h \sim 160-300$ μm[40]). For comparison, the anticipated time scale for antibody diffusing in a hydrated gel is ten times longer than $\tau_{rehydration}$, as $\tau_{diffusion} \sim h^2/D \sim 100$ s, where h is the height of the gel (~30 μm) and D is the diffusion coefficient for antibody in an 8% T gel.[41]

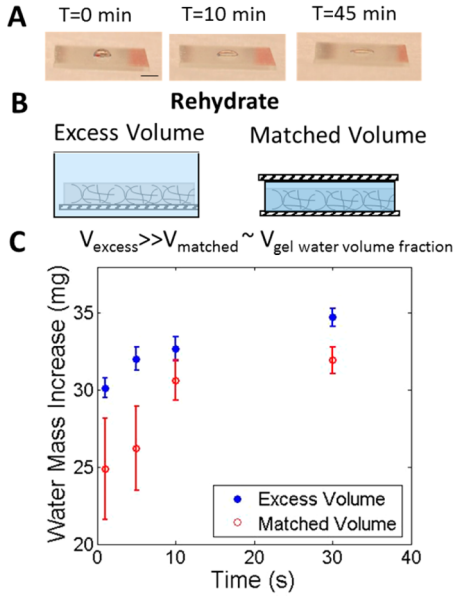

Figure 2. Hydration kinetics for determination of PA-liquid interfacing, and the volume of antibody solution required to match the hydrogel water volume fraction (A) Image of antibody droplet on the dry PA gel surface. Scale bar is 1 mm. (B) Schematic of PA gel slides were rehydrated in an excess volume of several milliliters of TBST (left) or with 50 μL of TBST which matches the gel hydration volume (right). (C) Change in mass of water in the gel upon rehydration for both rehydration methods (n = 3, error bar is standard deviation).

As a corollary consideration, the in-gel immunoassay using the dehydrated gels imposes the requirement that protein target (bound to the gel matrix) also be dehydrated. Previous crystallography and Fourier-transform infrared spectroscopy findings show that some proteins undergo irreversible conformation changes upon dehydration,[42,43] and the activity of dehydrated enzymes can decline significantly.[44] Our group has previously successfully demonstrated immunoprobing of scWB gels after gels were dried in a nitrogen stream and archived.[18,30] To multiplex protein target measurements, we rehydrated the gels, chemically stripped detection antibodies from the gels, and immunoprobed for new targets. We previously observed minimal change in immunoprobe signal (i.e., SNR of EGFP changed from 15 to 17 upon one stripping/reprobing cycle), suggesting protein dehydration did not hinder subsequent in-gel antibody binding.[18] Interestingly, the protein rehydration process is estimated to require ~4 min for water association with ionizable groups of an enzyme and >30 min for the complete water solvation shell to reform.[45] Thus, while we observed rapid antibody transport into the rehydrating gel, antibody binding may not occur immediately. Proteins may need time to rehydrate, which will depend on the gel dehydration state. Consequently, in this work, we adopted antibody probing times in line with our previous scWB assays for comparison (2 h and 1 h for primary and secondary antibody incubation, respectively).[18,30]

Characterization of Antibody Loading in Hydrated versus Dehydrated Gels. We utilized our procedure for drying and rehydrating the gel and developed a protocol to determine whether introducing detection antibody in the dehydrated gels increased the in-gel detection antibody concentration. We used a gel that did not have microwells and had no immobilized target protein (a blank gel). We

DOI: 10.1021/acs.analchem.5b03032
Anal. Chem. 2015, 87, 11030−11038

incubated the blank gel with fluorescently labeled detection antibody using either the "excess volume" or "matched volume" approaches (depicted with fluorescently labeled antibody solution in Figure 3A). The fluorescently labeled antibody

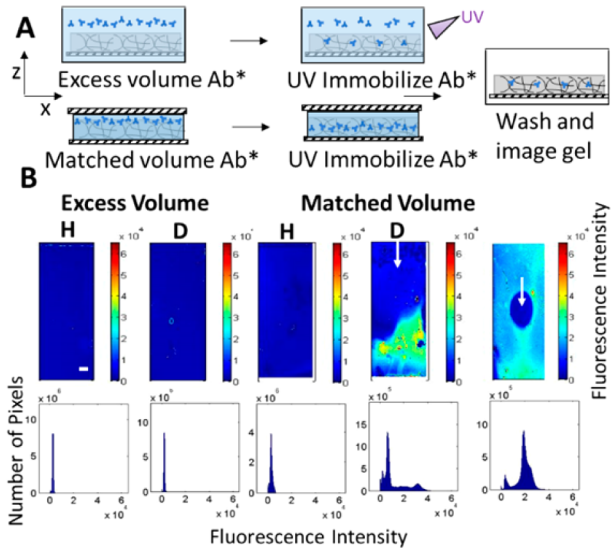

Figure 3. Detection of $[Ab^*]_{gel}$ in hydrated and dehydrated gels. (A) Schematic of excess volume (top row) and matched volume approaches to introduce antibody into gel. (B) Fluorescence intensity heat maps and fluorescence intensity histograms for hydrated (H) and dehydrated gels (D). White arrows indicate the location of antibody introduction in the hydration volume approach. Scale bar is 5 mm. Mean peak intensity in "excess volume" approach for hydrated and dehydrated gels were both 1627 ± 973 AFU (n = 3 gels, error reported is standard deviation). In the "matched volume" method the mean intensity in the hydrated gel was 2056 ± 630 A.F.U. (n = 4 gels) and the dehydrated gel was 8388 ± 2070 AFU (n = 4 gels), with a small second peak at 22738 ± 6802 AFU (n = 4 gels). When the droplet of antibody was added to the center of the gel the mean intensity was 25871 ± 11160 AFU (n = 6 gels), while the signal in the spot itself was 3104 ± 2107 AFU.

was immobilized in gel using UV-mediated benzophenone photocapture chemistry, as has been described and characterized previously.[34,41] Next, the gel was washed, dried and imaged. Imaging yielded a snapshot of the in-gel detection antibody concentration after incubation, with the important assumption that the UV immobilization was comparable in the hydrated and dehydrated gels. By drying the gel before imaging, we measured the in-gel antibody concentration eliminating out-of-plane fluorescence from a fluorescent liquid layer that would obscure the in-gel fluorescence. Probing using the "excess volume" method established the in-gel antibody concentration under well-characterized equilibrium partitioning behavior.[8]

To assess the increase in local detection antibody concentration (in the dehydrated gels compared to hydrated gels), we incubated and immobilized antibody utilizing the "matched volume" (from Figure 2) approach. Figure 3B shows that the mean antibody fluorescence intensity for the hydrated gel was within error of gels incubated in excess volume of antibody solution. In contrast, the mean antibody fluorescence intensity for the dehydrated gel was four times higher than the hydrated gel, with a second small peak in the intensity histogram that is 11 times higher than the hydrated gels. The 4−11 times higher antibody signal with the "matched volume" approach in dehydrated gels cannot be attributed to a change in the total liquid volume alone. Thus, we hypothesized the osmotic swelling pressure during rehydration[4] drives the solution of antibody into the gel. Finally, we observed the lowest signal at the gel location where the antibody solution first contacts the gel (see white arrows in Figure 3B). This suggests that spatial variation is associated with the dynamic process of rehydrating the dehydrated gel, a subject of continued investigation.

Since signal variation is large near the edge of the gel, as seen in Figure 3B, we sought to determine if gel edge defects impacted detection antibody transport through the gel. Thus, we investigated signal variation after depositing the droplet of antibody solution in the center of the gel and not near a gel edge. We observed the lowest antibody fluorescence signal (which was within error of the signal in the "excess volume" gels) at the location where the liquid first contacted the gel (Figure 3B). The mean antibody fluorescence intensity surrounding the center was ∼16 times higher than in the "excess volume" approach. Therefore, the observed nonuniformity did not correspond with gel edge defects, but rather from interfacing of the antibody solution with the gel. Of note, the nonuniform antibody introduction shown in Figure 3 poses a challenge to establishing a limit of detection for immunoprobing of a dehydrated gel containing known quantities of GFP (as was previously performed in scWB gels immunoprobed in the hydrated state, and shown to have a limit of detection of ∼27 000 copies of protein in the gel[18]). Future efforts to reduce spatial bias in the loading of antibody would allow for determination of this limit of detection in gels immunoprobed in the dehydrated state.

We attribute the observed nonuniformity to surface tension preventing spreading of the antibody droplet, thus leading to partitioning behavior where the antibody solution first contacts the gel. Gel hydration is a balance of the free energy of mixing from solvent−polymer interactions and the elastic free energy which opposes swelling.[46] However, this process did not occur initially because interfacial surface tension (Figure 2A) prevented spreading of the antibody droplet. The droplet volume exceeded the gel volume it contacted by 100×. Thus, before the antibody solution spread across the gel surface, the antibody droplet was effectively in the "excess volume" regime (at the location of the droplet), and "local partitioning" occurred. Diffusion of antibody to smooth the concentration gradient would require >200 days (assuming the nonuniformity is ∼10 mm characteristic diffusion length and the antibody diffusivity is as reported elsewhere[18]). Further experiments on the sensitivity of hydrogel loading to starting volume are warranted to determine if uniform macromolecule delivery to a dehydrated gel is feasible. Regardless, we have demonstrated a method of increasing the in-gel concentration of antibody (by ∼4−11 times) in a hydrogel without changing the composition of the gel or solute as other groups have demonstrated.[10−12] Thus, the "matched volume" approach for loading hydrogels with macromolecules may be generalizable to other in-gel immunoassays and drug delivery applications. For the latter, promising antibody therapies for cancer[47] may be realized with controlled release from hydrogels,[48] which could be loaded with the necessary dose by the "matched volume" approach described here.

Implications of Rehydration Time Scales and Local Antibody Concentration in Probing of Dehydrated Gels. To determine how the increased in-gel concentration of detection antibody attained with the "matched volume"

DOI: 10.1021/acs.analchem.5b03032
Anal. Chem. 2015, 87, 11030−11038

approach of antibody loading will affect the analytical sensitivity of a typical in-gel immunoassay, we developed a bimolecular binding kinetics model for antigen and antibody binding to form immunocomplex. The binding efficiency is defined as $C^* = [C]_{max}/[Ag]_0$, where $[C]_{max}$ was given in eq 2. We use a concentration of $[Ag]_0 = 0.75$ nM, which is just below the single-cell concentration of a median expressed protein,[49] as is relevant to our application of "matched volume" antibody loading for scWB immunoprobing. However, the model is broadly applicable, and may be used to inform design of other in-gel immunoassays as long as the approximate values for the variables in eq 2 are known. The binding efficiency is evaluated as a function of K_D (the ratio of k_{off}/k_{on}) in the 0.1−1 μM range assuming no mass transport limitations (the in-gel concentration of antibody instantaneously reaches the equilibrium concentration anticipated from Figure 3, "matched volume" approach). While the K_D of commercially available antibodies will vary widely depending on target antigen, most antibody isolated from naïve libraries will have K_D values in the micromolar range.[50] Certain in vivo isolation techniques can yield picomolar affinity antibodies.[51] Thus, the K_D range considered in Figure 4 is an estimate for low-to-moderate affinity antibodies.

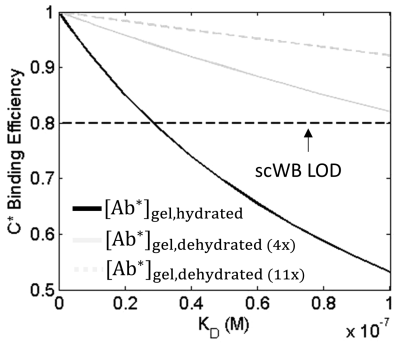

Figure 4. Binding kinetics model showing phase space where probing of dehydrated gels will improve scWB assay performance. The estimated in-gel antibody concentrations are based on the experiments in Figure 3 (with $[Ab^*]_0 = 6.7 \times 10^{-7}$ M, $K_{partition} = 0.17$, and the in-gel concentration in the dehydrated gels 4−11 times higher than the hydrated gels). The black dashed line is the previously reported scWB limit of detection (LOD).

As shown in Figure 4, the low concentration of antibody in the hydrated gel caused the binding efficiency to rapidly fall as a function of K_D. The concentration of antibody in the hydrated gel is estimated from Figure 3 using $K_{partition} = 0.17$, and the concentration of antibody in the matched volume data. Notably, at $K_D \approx 0.4 \times 10^{-7}$ M, detection antibody binding efficiency is below the previously reported LOD of the scWB.[18] In contrast, when the concentration of antibody corresponded with the 4−11x higher concentrations measured in the dehydrated gels using the matched volume approach (gray solid and dashed lines respectively in Figure 4), we found increased antibody concentration will drive immunocomplex formation above the LOD. Clearly, this improved sensitivity comes at the cost of increased measurement variance and binding efficiency variation that is K_D dependent. (Figure 3).

To increase model accuracy, we also consider any mass transport limitations on immunocomplex formation and, finally, in-gel immunoassay readout. We assessed such mass transport limitations on the assay by evaluating the Damköhler number of the system, which is defined as[52]

$$Da = \frac{\tau_{transport}}{\tau_{rxn}} \tag{3}$$

where τ_{rxn} is the reaction equilibration time

$$\tau_{rxn} = \frac{1}{k_{on}[Ab^*]_0 + k_{off}} \tag{4}$$

and $\tau_{transport}$ is the equilibration time for mass transport. For moderate-to-high affinity detection antibodies, any mass transport limitations will be exacerbated by the rapid reaction rates, so we consider $k_{on} \approx 10^4$−10^6 M^{-1} s^{-1} and the concentration of antibody estimated from our antibody incubation experiments. For hydrated gels, the diffusive equilibration time was ∼100 s. With an in-gel antibody concentration used in the kinetics model (Figure 4) we found $0.10 < Da < 10.0$, suggesting that the assay is largely mass transport limited. When dominated by mass transport limitations, assay time scales as the product of Da and the reaction equilibration time, and assay time increases.[15] In contrast in dehydrated gels, transport of antibodies (∼10 s) completes before the anticipated protein rehydration time (∼4 min[45]). The relevant antibody diffusion length scale once reactions can occur in this case is therefore the PA gel pore radius. This yields a reaction-limited assay ($2.3 \times 10^{-6} < Da < 2.4 \times 10^{-4}$). We anticipate probing of dehydrated gels could reduce assay duration, although further study is required to determine if protein-rehydration is a rate-limiting step.

Improved Antibody Probing Performance in Dehydrated Gels Compared with Hydrated Gels. To characterize the impact of increased local concentration of detection antibody in dehydrated gels in the scWB assay, we measured GFP in U373-Turbo GFP transfected cells. Robust characterization of assay variability utilizes direct correlation between the detection antibody signal and level of target protein immobilized on the PA gel. For direct measurement of target protein immobilization in this characterization study, we utilize signal from an expressed fluorescent protein (GFP). We compared probing efficiency in gels immunoprobed in the hydrated versus dehydrated state (Figure 5). When gels were immunoprobed in the dehydrated state, we observed both (1) a higher scWB immunoprobing signal (Figure 5A) and (2) a higher background signal (SI Figure 3), as compared to immunoprobing of gels in a hydrated state. We evaluated the A.U.C. for the bound detection antibody signal (immunocomplex, $[C]_{max}$) and normalized this A.U.C. to the expressed GFP A.U.C. ($[Ag]_0$) as a function of secondary antibody mass used ($[Ab]_0$, Figure 5B).

Strikingly, we found the median normalized A.U.C. for gels immunoprobed while dehydrated was ∼2−14 times higher than in gels immunoprobed while hydrated at all of the antibody masses utilized (Mann−Whitney U-test p-value < 0.00005 for each antibody mass used, Table S1; sample sizes reported in Table 1). Additionally, we observed higher signal-to-noise ratio (SNR) when antibody was introduced in the dehydrated gel at all antibody masses utilized (see Supporting Information), except at 0.25 μg (where the Mann−Whitney U-test p-value was higher than 0.05) and at 5 μg (where the median SNR was ∼1.4× higher for the gels immunoprobed in the hydrated state). To determine if the overlap of the SNR distributions with the 0.25 μg antibody mass was reproducible we performed

DOI: 10.1021/acs.analchem.5b03032
Anal. Chem. 2015, 87, 11030−11038

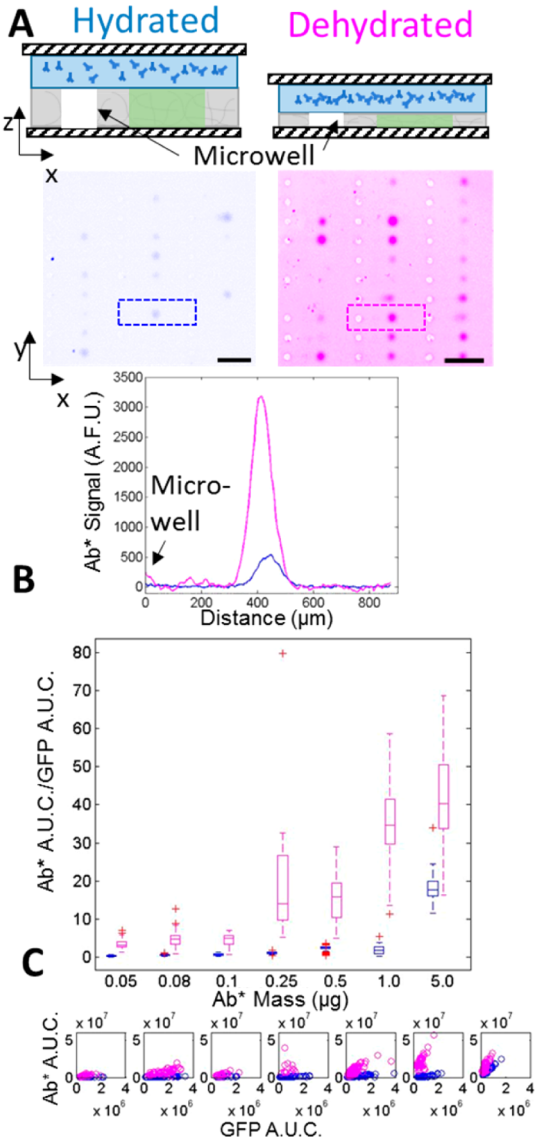

Figure 5. Increased scWB probing signal in dehydrated gels compared with hydrated gels. (A) Antibody fluorescence images and intensity plots of scWBs for GFP from U373-GFP cells in hydrated (left, blue) and dehydrated gels (right, magenta). Scale bar is 500 μm. (B) Antibody dilution dependence of area under the curve (AUC) values for the fluorescently labeled antibodies normalized to AUC for the expressed GFP. Horizontal line in the box is the median (higher for gels immunoprobed while dehydrated, Mann−Whitney U-test p-value <0.0005) and box edges are at 25th and 75th percentile. (C) Scatter plots of antibody AUC and GFP protein AUC for each detection antibody mass tested in B (scatter plot is below its corresponding box plot).

two replicates (shown in the Supporting Information). Again we found the SNR distributions overlapped (though the Mann−Whitney U-test p-value for the second replicate was $p < 0.05$). With application of 1 μg of detection antibody, we observed a maximum SNR in the gels immunoprobed in the dehydrated state (median SNR = 228.7) which was five-times higher than the median SNR of the gels immunoprobed in the hydrated state (median SNR = 43.6). The higher SNR in the gels that were dehydrated reflects an improved analytical sensitivity. Future work includes extending immunoprobing of dehydrated gels to measure low-abundance targets in single cells. Furthermore, we observed probing of dehydrated gels allows for up to 10-fold lower antibody consumption compared to hydrated gels. In Figure 5, we show nearly comparable median normalized A.U.C. for the gels immunoprobed in the dehydrated state utilizing 0.5 μg of antibody and the hydrated gel using 5 μg of Ab.

While the increased normalized A.U.C. and SNR show that probing dehydrated gels improved analytical sensitivity, we also observed high variation in the normalized A.U.C. when the gel was immunoprobed in the dehydrated state. For our gamma-distributed protein expression data[18,53] we required a metric of variance that accounts for skew of the distribution of protein expression. Thus, we used the coefficient of quartile variation, CQV,[54] which was developed to accurately describe variation in skewed distributions, and is defined as

$$\mathrm{CQV} = \frac{Q_3 - Q_1}{Q_3 + Q_1}$$

where Q_3 is the 75th percentile and Q_1 is the 25th percentile of the statistical distribution. The CQV of the normalized AUC was not dependent on the antibody mass used for immunoprobing hydrated or dehydrated gels (see table in Supporting Information for all CQV values and comparison with the coefficient of variation). The mean CQV across all antibody masses used was 26.1% ± 10.2% and 25.0% ± 17.2% for gels probed in the dehydrated and hydrated states respectively, meaning variation was comparable in the two methods. Further study of the contributions of technical variation in immunoprobing is important to identify technical versus biological variation in our measurement of cell-to-cell heterogeneity in protein expression.[18,30]

We sought to better understand the observed variance in immunoprobing by evaluating the correlation between antibody fluorescence and expressed GFP fluorescence. In Figure 5C and Table 1, we show the correlation between detection antibody A.U.C. and expressed GFP A.U.C. and calculated Pearson correlation coefficients, r, for the data in each scatter plot (Table 1). Ideally, the antibody signal would be directly linearly correlated with the expressed GFP signal ($r = 1$), though the highest observed r values were 0.97 and 0.8 for hydrated and

Table 1. Pearson Correlation Coefficients for Figure 5C[a]

antibody mass (μg)	0.05	0.08**	0.1	0.25**	0.5**	1	5**
hydrated Pearson r	r = 0.33*	r = 0.95*	r = 0.62*	r = 0.89*	r = 0.88*	r = 0.70*	r = 0.97*
	n = 50 cells	n = 78 cells	n = 78 cells	n = 58 cells	n = 165 cells	n = 64 cells	n = 74 cells
dehydrated Pearson r	r = 0.58*	r = 0.43*	r = 0.70*	r = −0.12 (p = 0.70)	r = 0.70*	r = 0.75*	r = 0.80*
	n = 43 cells	n = 48 cells	n = 23 cells	n = 12 cells	n = 162 cells	n = 23 cells	n = 47 cells

[a]Rejection of the null hypothesis that the correlation coefficient is zero indicated with * ($p < 0.003$). The rejection of the null hypothesis that the Pearson r of the hydrated gel is equivalent to the Pearson r of the dehydrated gel at a given antibody mass is indicated with ** ($p < 0.05$).

DOI: 10.1021/acs.analchem.5b03032
Anal. Chem. 2015, 87, 11030−11038

dehydrated gels, respectively. To determine whether the measured correlation coefficients were statistically the same between gels immunoprobed in the dehydrated and hydrated states, we utilized a Fisher's r to Z transformation[55] and a two-tailed Z-test. Correlation coefficients must be transformed to attain a normally distributed Z test statistic for which we can determine the p-value. At the 0.08, 0.25, 0.5, and 5 μg antibody masses, we rejected the null hypothesis that the Pearson r values in the hydrated and dehydrated gels were equivalent ($p < 0.05$), and we found the measured correlation coefficients were higher for gels immunoprobed while hydrated versus dehydrated. The lower correlation between antibody A.U.C. and expressed GFP A.U.C. for gels immunoprobed in the dehydrated state indicates increased technical variance associated with the measurement. We hypothesize the spatial variation in detection antibody introduction in dehydrated gels (Figure 3B) may contribute to the lower correlations between antibody A.U.C. and expressed GFP A.U.C. Further investigations will evaluate when increased technical variance might mask biological variance, as variance will be specific to the antibody, protein target, and biological system.

CONCLUSIONS

We report on rehydration of dehydrated hydrogels in sparing volumes of macromolecule solution for enhanced loading of a PA hydrogel. Our hydrogel is utilized for a single-cell immunoassay, which allows for detection of protein isoforms[18] and identification of off-target antibody binding unmeasurable in other single cell proteomic approaches used with cancer and stem cells.[19,33] By rehydrating the dehydrated scWB gel in a volume of antibody solution closely matched with the hydrogel water volume fraction, we achieved higher scWB immunoprobing signals and achieved reduced consumption of costly antibody reagents. This approach to mitigate partitioning presents a trade-off with antibody probing signal that may be less well-correlated with target protein levels. We anticipate the impact of this increased technical variation will be antibody affinity specific, and thus future work includes a survey of the impact of antibody affinity on technical variation in probing of hydrated versus dehydrated gels. Additionally, we observed an intriguing phenomena, whereby the region of the dehydrated gel that first made contact with the antibody solution yielded the lowest antibody fluorescence signal. Follow-up work could further characterize the hypothesized local partitioning effect, by measuring local antibody concentration as a function of the ratio of the antibody liquid volume and volume of the gel in contact with the antibody liquid. Given the straightforward nature of matched volume loading of macromolecule solutions in dehydrated gels, findings are relevant to numerous drug delivery and hydrogel assay applications.

ASSOCIATED CONTENT

Supporting Information

The Supporting Information is available free of charge on the ACS Publications website at DOI: 10.1021/acs.analchem.5b03032.

Analytical model of bimolecular binding kinetics (PDF)

AUTHOR INFORMATION

Corresponding Author

*E-mail: aeh@berkeley.edu.

Author Contributions

J.V. and A.E.H. designed the experiments. J.V. performed the cell culture and *sc*WBs. J.V. performed the data analysis. All authors wrote the manuscript. All authors have given approval to the final version of the manuscript.

Notes

The authors declare the following competing financial interest(s): J.V. and A.E.H. are inventors on pending patents related to scWB blot methods. A.E.H. holds equity interest in scWB commercialization efforts.

ACKNOWLEDGMENTS

This work was supported by an NIH New Innovator Award (No. DP2OD007294, to A.E.H.) and a National Science Foundation CAREER award (CBET-1056035 to A.E.H.). A.E.H. is an Alfred P. Sloan Foundation Research Fellow in Chemistry. J.V. was supported by a National Science Foundation Graduate Research Fellowship (DGE 1106400). The authors are grateful for helpful discussions with Dr. Augusto Tentori, Ms. Elisabet Rosas, Mr. Kevin Yamauchi, Dr. Ting Xu, Dr. Evelyn Wang, and Dr. Clay Radke.

REFERENCES

(1) Peppas, N. A.; Hilt, J. Z.; Khademhosseini, A.; Langer, R. *Adv. Mater.* **2006**, *18*, 1345−1360.
(2) Gupta, P.; Vermani, K.; Garg, S. *Drug Discovery Today* **2002**, *7*, 569−579.
(3) Hitzbleck, M.; Delamarche, E. *Chem. Soc. Rev.* **2013**, *42*, 8494.
(4) Hoffman, A. S. *Adv. Drug Delivery Rev.* **2002**, *54*, 3−12.
(5) Appleyard, D.; Chapin, S.; Doyle, P. *Anal. Chem.* **2011**, *83*, 193−199.
(6) Li, H.; Leulmi, R. F.; Juncker, D. *Lab Chip* **2011**, *11*, 528−534.
(7) De Lange, V.; Binkert, A.; Vörös, J.; Bally, M. *ACS Appl. Mater. Interfaces* **2011**, *3*, 50−57.
(8) Tong, J.; Anderson, J. L. *Biophys. J.* **1996**, *70*, 1505−1513.
(9) Gehrke, S. H.; Fisher, J. P.; Palasis, M.; Lund, M. E. *Ann. N. Y. Acad. Sci.* **1997**, *831*, 179−207.
(10) Gehrke, S. H.; Uhden, L. H.; McBride, J. F. *J. Controlled Release* **1998**, *55*, 21−33.
(11) Sivars, U.; Tjerneld, F. *Biochim. Biophys. Acta, Gen. Subj.* **2000**, *1474*, 133−146.
(12) Lewus, R. K.; Carta, G. *Ind. Eng. Chem. Res.* **2001**, *40*, 1548−1558.
(13) Albro, M. B.; Chahine, N. O.; Li, R.; Yeager, K.; Hung, C. T.; Ateshian, G. A. *J. Biomech.* **2008**, *41*, 3152−3157.
(14) Shalaby, W. S. W.; Abdallah, A. A.; Park, H.; Park, K. *Pharm. Res.* **1993**, *10*, 457−460.
(15) Squires, T. M.; Messinger, R. J.; Manalis, S. R. *Nat. Biotechnol.* **2008**, *26*, 417−426.
(16) Le Goff, G. C.; Srinivas, R. L.; Hill, W. A.; Doyle, P. S. *Eur. Polym. J.* **2015**, DOI: 10.1016/j.eurpolymj.2015.02.022.
(17) Moorthy, J.; Burgess, R.; Yethiraj, A.; Beebe, D. *Anal. Chem.* **2007**, *79*, 5322−5327.
(18) Hughes, A. J.; Spelke, D. P.; Xu, Z.; Kang, C.-C.; Schaffer, D. V.; Herr, A. E. *Nat. Methods* **2014**, *11*, 749−755.
(19) Burry, R. W. *J. Histochem. Cytochem.* **2011**, *59*, 6−12.
(20) Ng, A. H. C.; Dean Chamberlain, M.; Situ, H.; Lee, V.; Wheeler, A. R. *Nat. Commun.* **2015**, *6*, 7513.
(21) Perfetto, S. P.; Chattopadhyay, P. K.; Roederer, M. *Nat. Rev. Immunol.* **2004**, *4*, 648−655.
(22) Shapiro, H. M. Overture. In *Practical Flow Cytometry*; Blair, O. C., Ed.; John Wiley & Sons: Hoboken, NJ, 2003; pp 1−60.
(23) Bandura, D. R.; Baranov, V. I.; Ornatsky, O. I.; Antonov, A.; Kinach, R.; Lou, X.; Pavlov, S.; Vorobiev, S.; Dick, J. E.; Tanner, S. D. *Anal. Chem.* **2009**, *81*, 6813−6822.

DOI: 10.1021/acs.analchem.5b03032
Anal. Chem. 2015, 87, 11030−11038

(24) Fredriksson, S.; Gullberg, M.; Jarvius, J.; Olsson, C.; Pietras, K.; Gústafsdóttir, S. M.; Ostman, A.; Landegren, U. *Nat. Biotechnol.* **2002**, *20*, 473−477.
(25) Shi, Q.; Qin, L.; Wei, W.; Geng, F.; Fan, R.; Shin, Y. S.; Guo, D.; Hood, L.; Mischel, P. S.; Heath, J. R. *Proc. Natl. Acad. Sci. U. S. A.* **2012**, *109*, 419−424.
(26) Lu, Y.; Chen, J. J.; Mu, L.; Xue, Q.; Wu, Y.; Wu, P.-H.; Li, J.; Vortmeyer, A. O.; Miller-Jensen, K.; Wirtz, D.; Fan, R. *Anal. Chem.* **2013**, *85*, 2548−2556.
(27) Chambers, I.; Silva, J.; Colby, D.; Nichols, J.; Nijmeijer, B.; Robertson, M.; Vrana, J.; Jones, K.; Grotewold, L.; Smith, A. *Nature* **2007**, *450*, 1230−1234.
(28) Michel, M. C.; Wieland, T.; Tsujimoto, G. *Naunyn-Schmiedeberg's Arch. Pharmacol.* **2009**, *379*, 385−388.
(29) Egelhofer, T. A.; Minoda, A.; Klugman, S.; Lee, K.; Kolasinska-Zwierz, P.; Alekseyenko, A. A.; Cheung, M.-S.; Day, D. S.; Gadel, S.; Gorchakov, A. A.; Gu, T.; Kharchenko, P. V.; Kuan, S.; Latorre, I.; Linder-Basso, D.; Luu, Y.; Ngo, Q.; Perry, M.; Rechtsteiner, A.; Riddle, N. C.; Schwartz, Y. B.; Shanower, G. A.; Vielle, A.; Ahringer, J.; Elgin, S. C. R.; Kuroda, M. I.; Pirrotta, V.; Ren, B.; Strome, S.; Park, P. J.; Karpen, G. H.; Hawkins, R. D.; Lieb, J. D. *Nat. Struct. Mol. Biol.* **2011**, *18*, 91−93.
(30) Kang, C.-C.; Lin, J.-M. G.; Xu, Z.; Kumar, S.; Herr, A. E. *Anal. Chem.* **2014**, *86*, 10429−10436.
(31) Jøssang, T.; Feder, J.; Rosenqvist, E. *J. Protein Chem.* **1988**, *7*, 165−171.
(32) Holmes, D. L.; Stellwagen, N. C. *Electrophoresis* **1991**, *12*, 612−619.
(33) Maecker, H. T.; Trotter, J. *Cytometry, Part A* **2006**, *69*, 1037−1042.
(34) Dormán, G.; Prestwich, G. D. *Biochemistry* **1994**, *33*, 5661−5673.
(35) Shapiro, A. L.; Viñuela, E.; Maizel, J. V., Jr. *Biochem. Biophys. Res. Commun.* **1967**, *28*, 815−820.
(36) Scherer, G. W. *J. Non-Cryst. Solids* **1992**, *147−148*, 363−374.
(37) Gehrke, S. *Responsive Gels: Volume Transitions II* **1993**, *110*, 81−144.
(38) Baselga, J.; Hernández-Fuentes, I.; Masegosa, R. M.; Llorente, M. A. *Polym. J.* **1989**, *21*, 467−474.
(39) Toomey, R.; Freidank, D.; Rühe, J. *Macromolecules* **2004**, *37*, 882−887.
(40) Yoon, J.; Cai, S.; Suo, Z.; Hayward, R. C. *Soft Matter* **2010**, *6*, 6004.
(41) Hughes, A. J.; Lin, R. K. C.; Peehl, D. M.; Herr, A. E. *Proc. Natl. Acad. Sci. U. S. A.* **2012**, *109*, 5972−5977.
(42) Mirsky, A. E.; Pauling, L. *Proc. Natl. Acad. Sci. U. S. A.* **1936**, *22*, 439−447.
(43) Prestrelski, S. J.; Tedeschi, N.; Arakawa, T.; Carpenter, J. F. *Biophys. J.* **1993**, *65*, 661−671.
(44) Carpenter, J. F.; Crowe, J. H.; Arakawa, T. *J. Dairy Sci.* **1990**, *73*, 3627−3636.
(45) Daniel, R. M.; Dunn, R. V.; Finney, J. L.; Smith, J. C. *Annu. Rev. Biophys. Biomol. Struct.* **2003**, *32*, 69−92.
(46) Flory, P. J. *Principles of Polymer Chemistry*; Cornell University: Ithaca, NY, 1953.
(47) Scott, A. M.; Wolchok, J. D.; Old, L. J. *Nat. Rev. Cancer* **2012**, *12*, 278−287.
(48) Schweizer, D.; Serno, T.; Goepferich, A. *Eur. J. Pharm. Biopharm.* **2014**, *88*, 291−309.
(49) Li, J. J.; Bickel, P. J.; Biggin, M. D. *PeerJ* **2014**, *2*, e270.
(50) Yau, K. Y. F.; Dubuc, G.; Li, S.; Hirama, T.; Mackenzie, C. R.; Jermutus, L.; Hall, J. C.; Tanha, J. *J. Immunol. Methods* **2005**, *297*, 213−224.
(51) Batista, F. D.; Neuberger, M. S. *Immunity* **1998**, *8*, 751−759.
(52) Probstein, R. F. *Physicochemical Hydrodynamics: An Introduction*; John Wiley & Sons: New York, 2005.
(53) Friedman, N.; Cai, L.; Xie, X. S. *Phys. Rev. Lett.* **2006**, *97*, 168302.
(54) Bonett, D. G. *Comput. Stat. Data Anal.* **2006**, *50*, 2953−2957.
(55) Fisher, R. A. *Biometrika* **1915**, *10*, 507−521.

DOI: 10.1021/acs.analchem.5b03032
Anal. Chem. 2015, 87, 11030−11038

Effect of polymer hydration state on in-gel immunoassays

Julea Vlassakis[†,‡] and Amy E. Herr[*,†,‡]

†Department of Bioengineering and ‡The UC Berkeley/UCSF Graduate Program in Bioengineering, University of California Berkeley, Berkeley, California 94720, United States.

Supplementary Figure 1. Binding kinetics of complex formation at antibody concentrations anticipated in immunoprobing of hydrated gels.

Supplementary Figure 2. Binding kinetics of complex formation at with approximately five-times higher local concentration of detection antibody in the gel for immunoprobing.

Supplementary Figure 3. Boxplots of fluorescent detection antibody background and signal-to-noise ratio (SNR) from U373-GFP scWBs with immunoprobing of hydrated and dehydrated gels at various antibody masses.

Supplementary Figure 4. Boxplot of fluorescent detection antibody signal-to-noise ratio (SNR) from replicates of U373-GFP scWBs with immunoprobing of hydrated and dehydrated gels and heatmaps of SNR across the gel array.

Table S1: Summary of quantitation of median A.U.C. and metrics of variability from Fig. 5b. D corresponds to immunoprobing of dehydrated gels and H is immunoprobing of hydrated gels.

Analytical Model of Bimolecular Binding Kinetics

The binding kinetics model utilized in Results and Discussion is described here. Antibody-antigen binding to form immunocomplex, C, is governed by the following equilibrium reaction with forward rate constant k_{on} and backward rate constant k_{off}.

$$[Ab^*]_{gel} + [Ag]_0 \rightleftharpoons [C]$$

From bimolecular or Langmuir binding kinetics the concentration [C] as a function of time is given as:

$$[C] = [C]_{max}(1 - e^{-(k_{on}[Ab^*]_{gel} + k_{off})t})$$

where $[C]_{max}$ is the maximum complex concentration and is given by:

$$[C]_{max} = \frac{k_{on}[Ab^*]_{gel}[Ag]_0}{k_{on}[Ab^*]_{gel} + k_{off}}$$

For the anticipated partition coefficient K=0.17 for detection antibody in an 8%T gel, we show the complex concentration normalized to the starting antigen concentration as a function of time in Fig. S1, below. The equilibrium antibody-antigen complex concentration is expected to be 90% of saturation with a K_D of 10 nM at 1:10 dilution of 1 mg/mL antibody, and 1 nM antigen in gel (given the losses during scWB this would be a median expressed mammalian protein). Only 50% of saturated binding is achieved with a K_D of 100 nM (see Fig. S1-S2). With just a 5 times higher local antibody concentration in gel can drive reaction to 98% and 85% saturation respectively (Fig. S2), so clearly increasing local Ab concentration is important goal for analytical sensitivity.

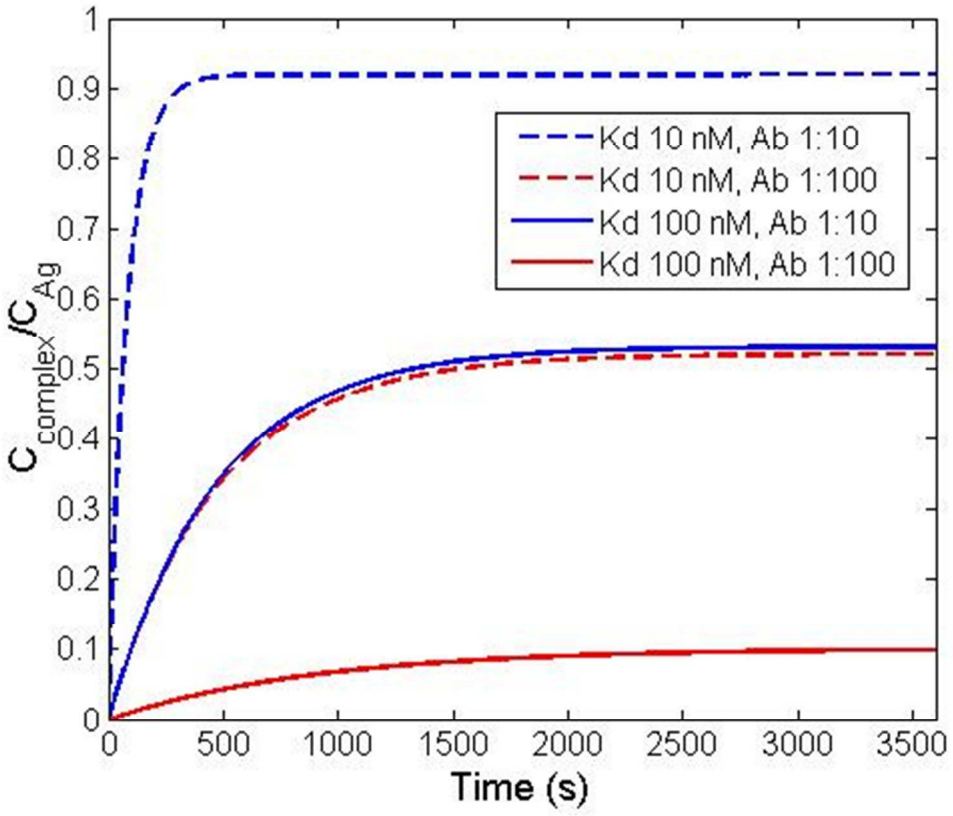

SI 1: Analytical kinetics model of antibody-antigen binding assuming ideal transport with a partition coefficient of 0.17 for the Ab in the PA gel. Antigen concentration $[Ag]_0$=1 nM, $k_{off}=10^{-3}s^{-1}$and $k_{on}=10^5M^{-1}s^{-1}$ or $10^4M^{-1}s^{-1}$. Antibody concentrations are $[Ab^*]_{gel}=6.7x10^{-7}$ M for 1:10 and $6.7x10^{-8}$ M for 1:100.

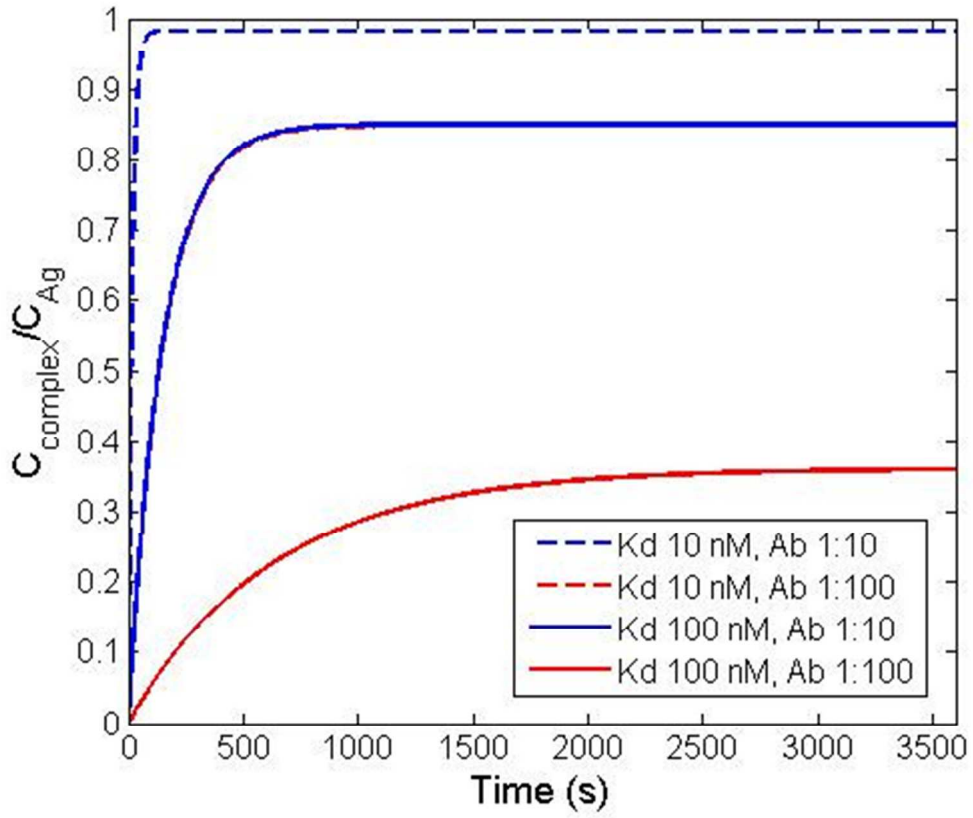

SI 2: Analytical kinetics model of antibody-antigen binding assuming ideal transport with a partition coefficient of 0.85 for the antibody in the PA gel. Antigen concentration $[Ag]_0$=1 nM, $k_{off}=10^{-3}s^{-1}$and $k_{on}=10^{5}M^{-1}s^{-1}$ or $10^{4}M^{-1}s^{-1}$. Ab concentrations are $[Ab^{*}]_{gel}=6.7x10^{-7}$ M for 1:10 and $6.7x10^{-8}$.

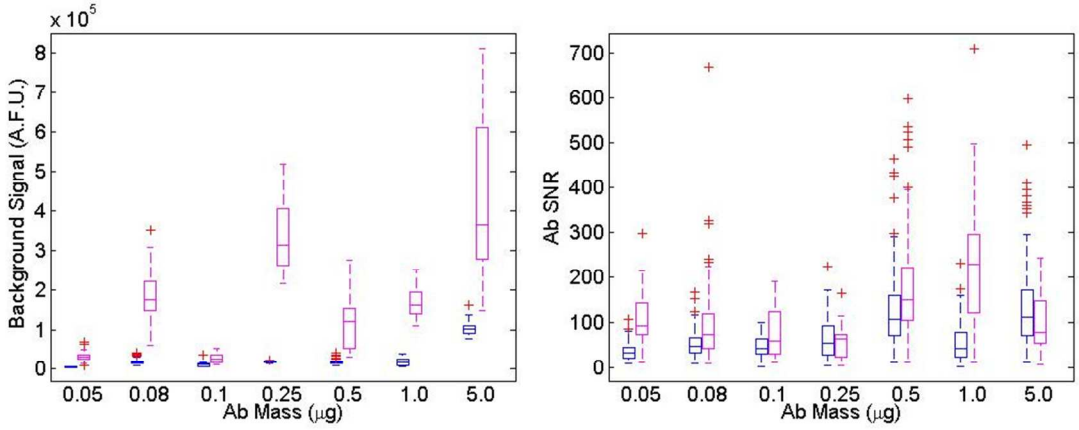

Fig. SI 3: Background signal and signal-to-noise ratio (SNR) of the fluorescent detection antibody signal from the same results depicted in main text Fig. 5. For the SNR, Mann-Whitney U test p-value<0.05 for all Ab masses except 0.25 μg. The background region was chosen as 3-4 standard deviations away from the peak center. Results indicate that wash-out of the detection

antibody was less effective in the dehydrated gels. Though the background signal was higher in gels immunoprobed in the dehydrated state (magenta) versus the hydrated state (blue), this did not impact the specificity or selectivity of the assay, as the peak signal was always distinguishable from the background.

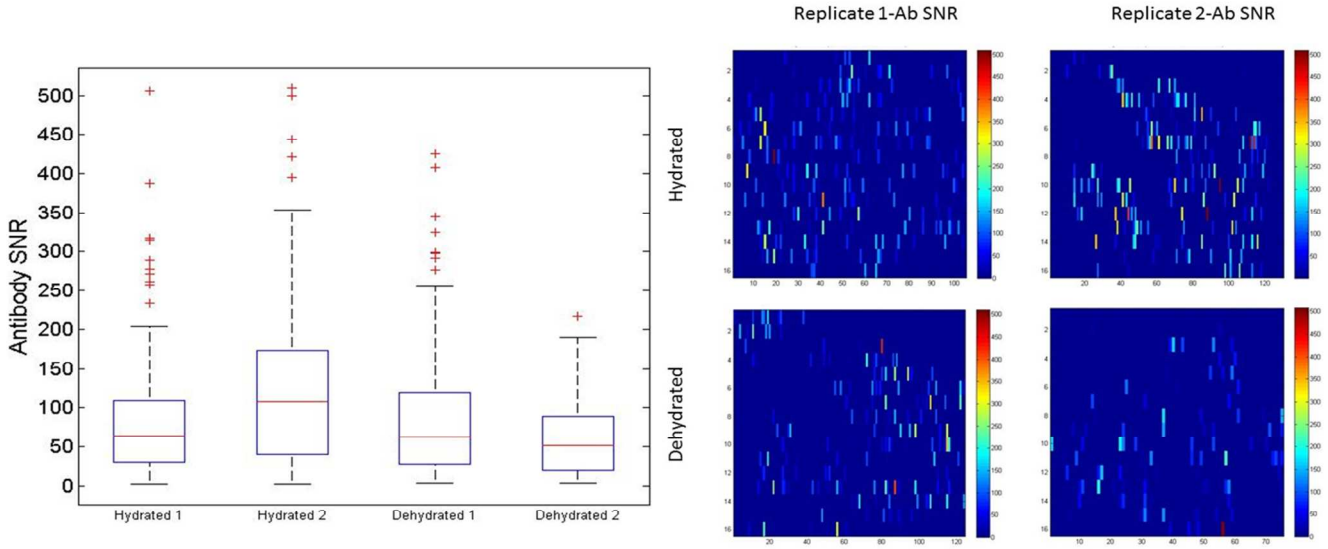

Fig. SI 4: Box plots and heatmaps showing detection antibody fluorescence SNR run-to-run variability in probing of gels in the hydrated versus dehydrated state. The replicates were collected at the 0.25 µg of Ab condition (where no statistically significant difference between SNR distributions for probing in hydrated or dehydrated gels was observed). Left: box plots of SNR for two replicates each of gels probed hydrated and dehydrated. The replicates performed with probing of dehydrated gels and hydrated gels yielded Mann-Whitney U test p-values of $p<0.05$, and $p<0.000005$ respectively. Thus we reject the null hypothesis that the distributions of the replicates are equivalent (inter-assay variability in SNR in gels immunoprobed with 0.25 µg of Ab is observed). The Mann-Whitney U test p-values comparing hydrated and dehydrated gels (e.g. hydrated 1 SNR vs. dehydrated 1 SNR, etc.) yielded $p>0.9$ and $p<0.05$ for replicates 1 and 2 respectively. Right: heatmaps showing spatial distribution of SNR in the replicates.

Table S1: Summary of quantitation of median AUC and metrics of variability from Fig. 5b. D corresponds to immunoprobing of dehydrated gels and H is immunoprobing of hydrated gels. The CV is the coefficient of variation.

Mass of Ab (µg)	Median A.U.C. (D)	Median A.U.C. (H)	CQV (D)	CQV (H)	CV (D)	CV (H)
0.05	3.0976	0.32503	20.35717	36.86089	35.478	45.595
0.083333	4.5943	0.48326	24.17221	14.59317	46.857	25.481
0.1	4.8139	0.64985	24.95586	33.28148	34.907	43.683
0.25	14.0011	1.0035	47.06971	15.38406	96.239	24.458
0.5	15.7653	2.3354	29.94712	9.076528	36.229	21.804
1	34.698	1.7587	16.66255	54.98288	28.421	64.111

5	40.3336	17.6025	19.98149	10.50667	29.04	18.138